# EXPERIMENTAL RESULTS ON OUTPUT-FEEDBACK CONTROL OF A NONSMOOTH ROTOR DYNAMIC SYSTEM

**J.C.A. de Bruin, A. Doris, N. van de Wouw, H. Nijmeijer**

*Department of Mechanical Engineering*
*Technische Universiteit Eindhoven*
*P.O. Box 513, NL 5600 MB Eindhoven*
*The Netherlands*
*J.C.A.de.Bruin@tue.nl, A.Doris@tue.nl,*
*N.v.d.Wouw@tue.nl, H.Nijmeijer@tue.nl*

Abstract: An experimental implementation of an output-feedback controller on a rotor dynamic system with set-valued friction is presented. The system exhibits coexisting stable/unstable equilibria and undesired friction-induced limit cycles. In the system, the friction and actuation are non-collocated, which prevents the application of standard friction compensation techniques. Therefore, an output-feedback control strategy is proposed that eliminates the friction-induced limit cycling, stabilizes the desired equilibrium and is robust for uncertainties in the friction model. The effectiveness of the proposed control strategy is shown both in simulations and experiments. 

Keywords: Setpoint control, Discontinuous systems, Set-valued friction, Limit cycles.

## 1. INTRODUCTION

In this paper, the experimental results of an output-feedback control design suppressing friction-induced limit cycling in a rotor dynamic system are presented. The rotor dynamic system consists of an actuated inertia which is connected to a second inertia with a low-stiffness link. The second inertia is subject to friction which is described by a model that contains dry friction and the Stribeck effect or so-called negative damping (Olsson *et al.*, 1998). The Stribeck effect gives rise to unstable equilibria and stable periodic responses (limit cycles) of the rotor dynamic system, where the equilibria reflect constant rotational velocity solutions of both inertias.
Extensive research has been performed with respect to the experimental rotor dynamic set-up under study. The modeling, parameter estimation and analysis of the dynamic behaviour of the set-up are discussed in (Mihajlović *et al.*, 2004; Mihajlović *et al.*, 2006).

It is important to note that the examined system configuration and control problem considered here, are encountered in many industrial rotor dynamic systems, such as drilling systems for oil exploration, see e.g. (Leine *et al.*, 2002), drivelines of sea ships, printers etc. In such engineering systems, limit cycling is an undesirable phenomenon because it causes kinetic energy dissipation, noise, excessive wear of machine parts and inferior positioning properties. Research on friction-induced limit cycling in different mechanical systems has been conducted in e.g. (Olsson and Åström, 2001; Jeon and Tomizuka, 2005; Mallon *et al.*, 2006).

The goal is to control the rotor dynamic system to a stable, constant velocity, equilibrium (thereby eliminating limit cycling). Note that in many rotor dynamic engineering systems, such as drilling systems, such constant velocity solution represents the desired operating steady-state. The main difficulty in attaining this goal is that the second inertia is not actuated and the modeled friction at the second inertia is set-valued. Due to the non-collocated nature of the friction and actuation, standard techniques (Armstrong-Hélouvry *et al.*, 1994; Mallon *et al.*, 2006) can not be employed for friction compensation. b In the literature, results on the control of nonsmooth systems with non-collocation of actuation and dry friction are limited. Integrator backstepping can be used for nonsmooth systems to stabilize the equilibrium (Tanner and Kyriakopoulos, 2003). This approach is based on nonsmooth analysis and Lyapunov stability for nonsmooth systems and its application is limited to systems in strict-feedback form. A variable structure control design is presented in (Kwatny *et al.*, 2002) for systems to deal with nonsmooth uncertainties. A variable structure controller is designed by using a multi-state backstepping procedure. However, the intended application is to systems where uncertain friction forces are relatively small. Trajectory control for systems with non-collocated actuation and nonsmooth friction by a model adaptive reference control scheme is studied in (Taware *et al.*, 2003). The model reference adaptive scheme uses static feedback for control and dynamic output feedback for parameter adaptation to achieve output tracking.

The mentioned control strategies for nonsmooth systems use the full state of the system to stabilize the equilibrium or to achieve output tracking. In this work, the experimental validation of the stabilization of equilibria is shown for a nonsmooth rotor dynamic system via output feedback. The control design is based on the Popov criterion, which results in robustness with respect to set-valued nonlinearities in the system. Control design based on the circle criterion and the Popov criterion for (nonlinear) continuous systems are discussed in e.g. (Arcak *et al.*, 2003). In the current work, the control design based on the Popov criterion is extended for application to nonsmooth rotor dynamic systems. The focus of this paper is on the experimental implementation and validation of this control strategy.

The paper is organized as follows. The experimental set-up is described in Section 2 where also the model of the system is presented. The output-feedback controller is introduced in Section 3. In Section 4, both simulation and experimental results are discussed to illustrate the effectiveness of the control strategy. The paper is finished with the conclusions in Section 5.

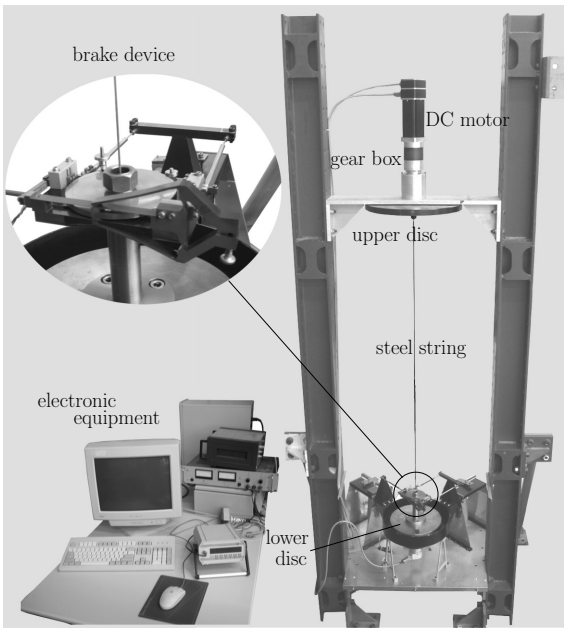


Fig. 1. Photo of the rotor dynamic set-up.

## 2. EXPERIMENTAL SET-UP

The experimental set-up consists of an upper disc driven by a drive part (consisting of a power amplifier, DC-motor and a gear box), a steel string, a lower disc and a brake device, see Figure 1. The upper disc is connected to the lower disc by a steel string, which is a low-stiffness connection between the discs. A brake disc is connected to the lower disc and a brake device is attached to the brake disc to exert a normal force to it. Oil is supplied to the brake disc to create an oil layer between the disc and the brake device. This combination of the brake device with lubrication creates a friction characteristic with Stribeck effect or with a so-called negative damping characteristic. Two incremental encoders are used to measure the angular positions of the lower and the upper discs.

A schematic representation of the rotor dynamic system is depicted in Figure 2. The drive part of the rotor dynamic system is considered as a single component for the modeling of the rotor dynamic set-up and where $u$ is defined as the input voltage to the drive part.

The system has two degrees of freedom; the upper disc and lower disc both have rotational freedom. The equations of motion for the upper disc and the lower disc are given by

$$\begin{aligned} J_u\ddot{\theta}_u + k_\theta(\theta_u - \theta_l) + T_{fu}(\dot{\theta}_u) - k_m u = 0 \\ J_l\ddot{\theta}_l - k_\theta(\theta_u - \theta_l) + T_{fl}(\dot{\theta}_l) = 0, \end{aligned} \tag{1}$$

with $\theta_u$ the angular position of the upper disc and $\theta_l$ the angular position of the lower disc. Set-

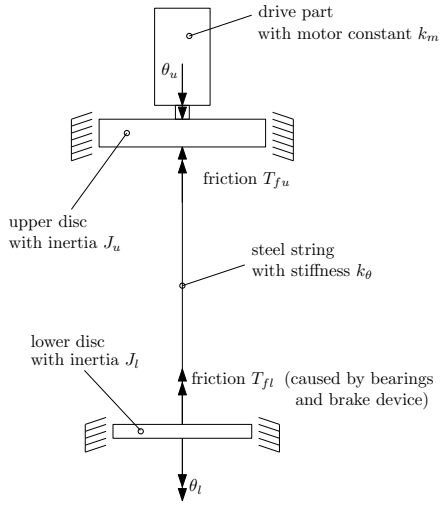


Fig. 2. Schematic drawing of rotor system.

valued force laws are used to model the friction acting on the upper and lower disc to account for the sticking effect in both characteristics. The friction acting on the upper disc is caused by the electromagnetic field in the drive part and the bearings that support the disc and is modeled by $T_{fu}$, see Figure 3:

$$T_{fu}(\dot{\theta}_u) \in \begin{cases} T_{cu}(\dot{\theta}_u)\mathrm{sgn}(\dot{\theta}_u) & \text{for } \dot{\theta}_u \neq 0 \\ [-T_{su}+\Delta T_{su}, T_{su}+\Delta T_{su}] & \text{for } \dot{\theta}_u = 0, \end{cases} \tag{2}$$

where the function $T_{cu}(\dot{\theta}_u)$ is given by

$$T_{cu}(\dot{\theta}_u) = T_{su} + \Delta T_{su}\mathrm{sgn}(\dot{\theta}_u) + b_u|\dot{\theta}_u| + \Delta b_u \dot{\theta}_u. \tag{3}$$

The friction $T_{fl}$ acting on the lower disc is caused by bearings that support the lower disc and, mainly, by the brake device. The friction $T_{fl}$, see Figure 4, is represented by

$$T_{fl}(\dot{\theta}_l) \in \begin{cases} T_{cl}(\dot{\theta}_l)\mathrm{sgn}(\dot{\theta}_l) & \text{for } \dot{\theta}_l \neq 0 \\ [-T_{sl}, T_{sl}] & \text{for } \dot{\theta}_l = 0, \end{cases} \tag{4}$$

and the continuous function $T_{cl}(\dot{\theta}_l)$ is given by

$$T_{cl}(\dot{\theta}_l) = T_{cl} + (T_{sl} - T_{cl})e^{-|\frac{\dot{\theta}_l}{\omega_{sl}}|^{\delta_{sl}}} + b_l|\dot{\theta}_l|. \tag{5}$$

The state-space equations of the rotor dynamic system are given by

$$\begin{aligned} \dot{x}_1 &= x_2 - x_3 \\ \dot{x}_2 &= \frac{1}{J_u}[-k_\theta x_1 - T_{fu}(x_2) + k_m u] \\ \dot{x}_3 &= \frac{1}{J_l}[k_\theta x_1 - T_{fl}(x_3)] \\ y &= x_1, \end{aligned} \tag{6}$$

where the state vector $x$ is defined as

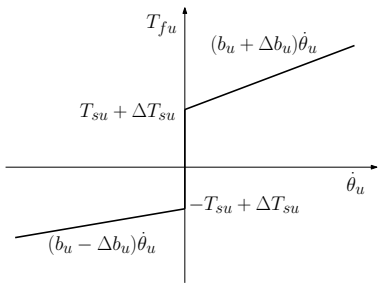


Fig. 3. Upper friction model $T_{fu}$.

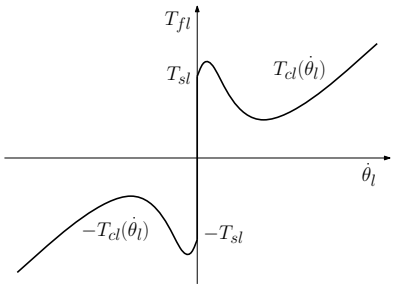


Fig. 4. Lower friction model $T_{fl}$.

$$x = \begin{bmatrix} x_1 \\ x_2 \\ x_3 \end{bmatrix} = \begin{bmatrix} \alpha \\ \omega_u \\ \omega_l \end{bmatrix} = \begin{bmatrix} \theta_u - \theta_l \\ \dot{\theta}_u \\ \dot{\theta}_l \end{bmatrix}. \tag{7}$$

Note that the state $\alpha = \theta_u - \theta_l$ represents the relative angular displacement of the lower disc with respect to the upper disc.
The system (6) can be written in a Lur'e-type form, which is convenient for the design of the output-feedback controller:

$$\begin{aligned} \dot{x} &= Ax + Gw + Bu \\ z &= Hx \\ w &\in -\varphi(z) \\ y &= Cx, \end{aligned} \tag{8}$$

where state $x \in \mathbb{R}^3$, $w, z \in \mathbb{R}^2$, input $u \in \mathbb{R}$, measured output $y \in \mathbb{R}$, and $\varphi(z) = [\varphi_1(z_1) \quad \varphi_2(z_2)]^T$ with $\varphi_i : \mathbb{R} \to \mathbb{R}$ for $i = 1, 2$. The matrices and the discontinuity $\varphi(z)$ in (8) are given by

$$A = \begin{bmatrix} 0 & 1 & -1 \\ -\frac{k_\theta}{J_u} & 0 & 0 \\ \frac{k_\theta}{J_l} & 0 & 0 \end{bmatrix}, B = \begin{bmatrix} 0 \\ \frac{k_m}{J_u} \\ 0 \end{bmatrix}, \tag{9}$$

$$G = \begin{bmatrix} 0 & 0 \\ \frac{1}{J_u} & 0 \\ 0 & \frac{1}{J_l} \end{bmatrix}, H = \begin{bmatrix} 0 & 1 & 0 \\ 0 & 0 & 1 \end{bmatrix}, \tag{10}$$

$$\varphi(z) = \begin{bmatrix} T_{fu}(z_1) \\ T_{fl}(z_2) \end{bmatrix}. \tag{11}$$

Table 1. Estimated parameters.

| parameter | value | unit |
|---|---|---|
| $k_m$ | 4.3228 | [Nm/V] |
| $J_u$ | 0.4765 | [kg m$^2$] |
| $T_{su}$ | 0.37975 | [Nm] |
| $\Delta T_{su}$ | -0.00575 | [Nm] |
| $b_u$ | 2.4245 | [kg m$^2$/rad s] |
| $\Delta b_u$ | -0.0084 | [kg m$^2$/rad s] |
| $k_\theta$ | 0.075 | [Nm/rad] |
| $J_l$ | 0.035 | [kg m$^2$] |
| $T_{sl}$ | 0.26 | [Nm] |
| $T_{cl}$ | 0.05 | [Nm] |
| $\omega_{sl}$ | 2.2 | [rad/s] |
| $\delta_{sl}$ | 1.5 | [-] |
| $b_l$ | 0.009 | [kg m$^2$/rad s] |

The parameters of the rotor dynamic model (6) are estimated by dedicated parameter identification experiments, following a similar procedure as described in (Mihajlović *et al.*, 2004). The estimation procedure is a delicate process, since the friction acting on the lower disc is very sensitive to conditions such as temperature, humidity and the lubrication conditions. The control goal is to stabilize the equilibria of the rotor dynamic system. Therefore, a predictive model is desired for the steady-state behaviour of the rotor dynamic system. The estimated parameters are validated by comparing the steady-state solutions of the simulations with those of the experiments. The estimated parameters are summarized in Table 1. The reader is referred to (Mihajlović *et al.*, 2006) for an extensive investigation of the analysis of the dynamic behaviour of the rotor dynamic system.

Next, a bifurcation diagram for the rotor dynamic system is presented with the constant input voltage $u_c$ as the bifurcation parameter. The different (co-existing) steady-state solutions of the rotor dynamic system are depicted in the bifurcation diagram for a constant input voltage $u_c$, see Figure 5. The results from the experiments are represented by marks and the results of the simulations by lines. The maximum and minimum value of the state $\omega_l$ are plotted in the bifurcation diagram in case the response is a periodic solution. For the region with constant input voltages up to approximately $u_c = 2.7$ V, only stable limit cycles are observed. Figure 6 shows such a limit cycle response for $u_c = 2.7$ V. In the region with input voltages from approximately 2.7 V up to approximately 4.5 V, two stable steady-state solutions co-exist. In this region, the steady-state solution can be either an equilibrium point or a stick-slip limit cycle depending on the initial conditions. For constant input voltages higher than 4.5 V, only a stable equilibrium point occurs. The control goal is to stabilize the unstable equilibria up to $u_c = 2.7$ V and to eliminate the limit cycles up to 4.5 V.

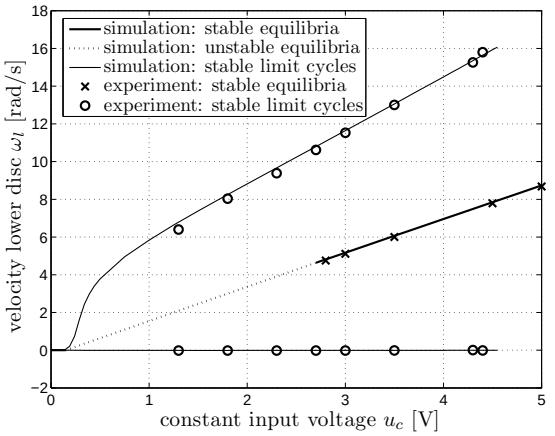


Fig. 5. Bifurcation diagram for open-loop rotor dynamic system.

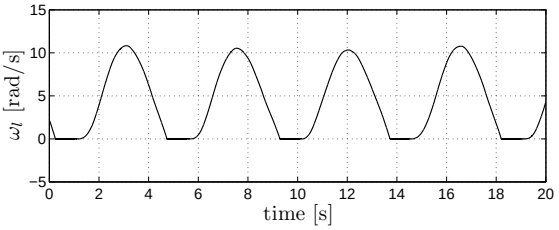


Fig. 6. Experimental limit cycle response of the rotor dynamic system for $u_c = 2.7$ V.

## 3. OUTPUT-FEEDBACK CONTROLLER

The control strategy presented in this section aims at rendering the isolated constant velocity equilibria of the open-loop system (8) globally asymptotically stable, thereby eliminating the unwanted stick-slip limit cycling. The output-feedback controller exploits the estimated state of the rotor dynamic system obtained from an observer. The proposed observer (Juloski *et al.*, 2006) for the rotor dynamic system (6) is given by

$$\begin{cases} \dot{\hat{x}} = A\hat{x} + L(y - C\hat{x}) + G\hat{w} + Bu \\ \hat{w} \in -\varphi(\hat{z}) \\ \hat{z} = H\hat{x} + N(y - C\hat{x}) \\ \hat{y} = C\hat{x}, \end{cases} \tag{12}$$

where the rotor dynamic state estimate $\hat{x} \in \mathbb{R}^3$, $\hat{z}, \hat{w} \in \mathbb{R}^2$, $\hat{y} \in \mathbb{R}$ and the observer matrices $N \in \mathbb{R}^{2\times1}$, $L \in \mathbb{R}^{3\times1}$ are to be designed.
The output-feedback control law is given by

$$u = u_c + u_{comp} + K(\hat{x} - x_{eq}), \tag{13}$$

with $x_{eq} = [\alpha_{eq} \quad \omega_{eq} \quad \omega_{eq}]^T$ the desired equilibrium of the rotor dynamic system (8), the control gain $K \in \mathbb{R}^{1\times3}$ and

$$u_{comp} = \frac{1}{k_m}(T_{fu} - b_u\hat{x}_2). \tag{14}$$

The part $u_{comp}$ of the control law compensates partly the friction acting at the upper disc of the rotor dynamic system. The resulting 'effective' friction acting at the upper disc is purely viscous. Note that such a friction compensation can not be employed to compensate for the friction at the lower disc, which is responsible for the stick-slip limit cycling.
The application of the control law (13) to the rotor dynamic system (6) results in an interconnection of the observer error dynamics and the closed-loop rotor dynamic system. The observer error is defined as $e = x - \hat{x}$ and the interconnected system is then given by

$$\begin{aligned} \dot{x} &= (A+BK)x + Gw - BKe \\ &\quad -BKx_{eq} + Bu_c + Bu_{comp} \\ z &= Hx \\ w &\in -\varphi(z) \\ y &= Cx, \end{aligned} \tag{15a}$$

$$\begin{aligned} \dot{e} &= (A-LC)e + G(w-\hat{w}) \\ \hat{z} &= H\hat{x} + N(y - C\hat{x}) \\ \hat{w} &\in -\varphi(\hat{z}). \end{aligned} \tag{15b}$$

For computation of the observer gains $L, N$ and the control gain $K$ that guarantee global asymptotic stability of the equilibria $(x, e) = (x_{eq}, 0)$, a result is used presented in (de Bruin, 2006). For the sake of brevity and given the experimental focus of the current paper, the closed-loop stability proof is omitted here. Instead the conditions are presented that the closed-loop dynamics (15) should satisfy. In (de Bruin, 2006), it is shown that global asymptotic stability of equilibrium $(x, e) = (x_{eq}, 0)$ is guaranteed if:

(1) the equilibrium $e = 0$ of the observer error dynamics (15b) is globally exponentially stable,
(2) the equilibrium $x = x_{eq}$ of the closed-loop rotor dynamic system (15a) for $e = 0$ is globally asymptotically stable and,
(3) the state $x(t)$ in (15a) is bounded for any bounded input $e(t)$.

These conditions are satisfied when two matrix inequalities, implying strict passivity of the linear parts of (15a) and (15b), are satisfied by appropriately designing the control and observer gains and the nonlinearity $\varphi$ is linearly bounded and monotone. The nonlinearity $\varphi$ can be made monotone by means of a loop transformation. Moreover, additional robustness with respect to the nonlinearity $\varphi$ can be obtained by a loop transformation. The resulting gains are given by (de Bruin, 2006):

$$K^T = \begin{bmatrix} 15.9 \\ 1.57 \\ 27.6 \end{bmatrix}, L = \begin{bmatrix} 195 \\ -312 \\ -9080 \end{bmatrix}, N = \begin{bmatrix} -2.22 \\ -37.8 \end{bmatrix}. \tag{16}$$

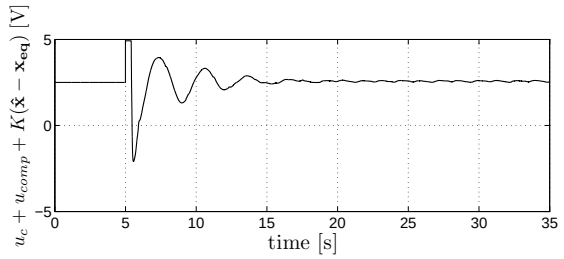


(a) Input voltage.

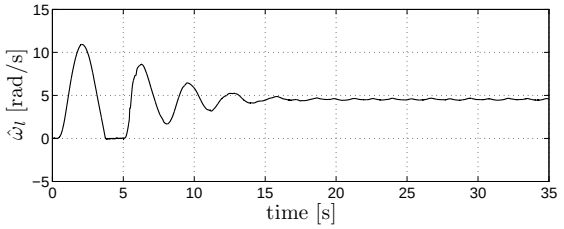


(b) Estimated velocity lower disc.

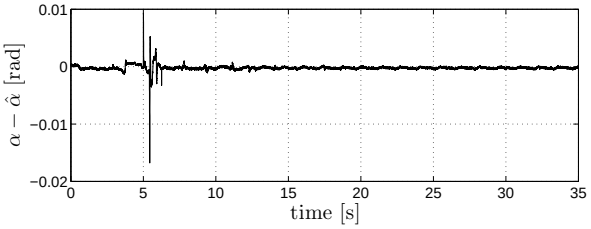


(c) Observer error (w.r.t. position difference upper and lower disc).

Fig. 7. Experimental closed-loop response of the rotor dynamic system for $u_c = 2.5$ V.

## 4. SIMULATIONS AND EXPERIMENTS

The presented output-feedback controller is applied to the rotor dynamic system. Note that the actuator input voltage of the rotor dynamic setup is limited to the range $[-5V, 5V]$. An additional low-pass filter is applied to the observed velocity of the lower disc to avoid undesired high-frequency phenomena (e.g. chatter) when the observed velocity of the lower disc is fed back to the controller.

The resulting output-feedback controller is used to stabilize the equilibria of the rotor dynamic setup for large range of constant inputs. The experimental closed-loop transient response is shown for the constant input voltage $u_c = 2.5$ V in Figure 7. For the open-loop rotor dynamic system (6), the only stable solution is a limit cycle, see Figure 5. The output-feedback controller is switched on at $t = 5$ s and the closed-loop system converges to the equilibrium state ($\alpha_{eq} = 1.36$ rad and $\omega_{eq} = 4.40$ rad/s). Note that the input voltage is saturated for approximately 0.5 seconds when the output-feedback controller is switched on. The saturation does, however, not influence the steady-state solutions.

Both experimental and model-based bifurcation diagrams for the closed-loop rotor dynamic sys-

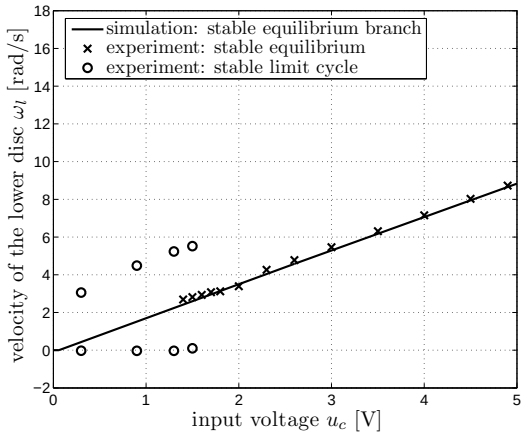


Fig. 8. Bifurcation diagram for closed-loop rotor dynamic system.

tem are depicted in Figure 8. The simulated bifurcation diagram shows that for all constant $u_c$ the desired equilibrium is globally asymptotically stabilized. In experiments, the output-feedback controller is able to eliminate the stable limit cycles and to stabilize the unstable equilibria for a large range of constant inputs $u_c$. However, for a small range of low voltages, the output-feedback controller can not stabilize the equilibria of the experimental rotor dynamic set-up. The remaining closed-loop limit cycles up to $u_c = 1.5$ V differ from the open-loop limit cycles. A cause for this lack of stability of the equilibria at these low input voltages may be some unmodeled position-dependent friction acting on the lower disc.

## 5. CONCLUSIONS

In this paper, a rotor dynamic system with set-valued friction is considered. The presence of friction causes undesirable stick-slip limit cycling. Due to the non-collocated nature of the friction and actuation, standard friction compensation techniques can not be used. Therefore, an output-feedback control strategy is proposed that stabilizes the unstable equilibria and eliminates the stick-slip limit cycles. The effectiveness of this strategy is shown in both simulations and experiments.

## REFERENCES


Arcak, M., M. Larsen and P. Kokotović (2003). Circle and Popov criteria as tools for nonlinear feedback design. *Automatica* **39**(4), 643–650.

Armstrong-Hélouvry, B., P. Dupont and C. Canudas de Wit (1994). A survey of models, analysis tools and compensation methods for the control of machines with friction. *Automatica* **30**(7), 1083–1138.

de Bruin, J.C.A. (2006). Control of systems with actuation and non-collocated discontinuous friction. Master's thesis. Technische Universiteit Eindhoven. Eindhoven.

Jeon, S. and M. Tomizuka (2005). Limit cycles due to friction forces in flexible joint mechanisms. In: *Proceedings of the 2005 IEEE/ASME International Conference on Advanced Intelligent Mechatronics*. Monterey, California, USA. pp. 723–728.

Juloski, A.L., N. Mihajlović, W.P.M.H. Heemels, N. van de Wouw and H. Nijmeijer (2006). Observer design for an experimental rotor system with discontinuous friction. *in Proceedings of the American Control Conference (ACC 2006)* pp. 2886–2891.

Kwatny, H.G., C. Teolis and M. Mattice (2002). Variable structure control of systems with uncertain nonlinear friction. *Automatica* **38**(7), 1251–1256.

Leine, R.I., D.H. van Campen and W.J.G. Keultjes (2002). Stick-slip whirl interaction in drillstring dynamics. *Journal of Vibration and Acoustics* **124**, 209–220.

Mallon, N., N. van de Wouw, D. Putra and H. Nijmeijer (2006). Friction compensation in a controlled one-link robot using reduced-order observer. *IEEE Transactions on Control Systems Technology* **14**(2), 374–383.

Mihajlović, N., A.A. van Veggel, N. van de Wouw and H. Nijmeijer (2004). Analysis of friction-induced limit cycling in an experimental drill-string system. *Journal of Dynamic Systems, Measurement and Control* **126**(4), 709–720.

Mihajlović, N., N. van de Wouw, M.P.M. Hendriks and H. Nijmeijer (2006). Friction-induced limit cycling in flexible rotor systems: an experimental drill-string set-up. *Nonlinear Dynamics* **46**(3), 273–291.

Olsson, H. and K.J. Åström (2001). Friction generated limit cycles. *IEEE Transactions on Control Systems Technology*.

Olsson, H., K. J. Åström, C. Canudas de Wit, M. Gafvert and P. Lischinsky (1998). Friction models and friction compensation. *European Journal of Control* **4**(3), 176–195.

Tanner, H.G. and K.J. Kyriakopoulos (2003). Backstepping for nonsmooth systems. *Automatica* **39**(7), 1259–1265.

Taware, A., G. Tao, N. Pradhan and C. Teolis (2003). Friction compensation for a sandwich dynamic system. *Automatica* **39**(3), 481–488.